NATIONAL ADVISORY COMMITTEE FOR AERONAUTICS

TECHNICAL MEMORANDUM 1355

STUDY OF THE SUPERSONIC PROPELLER

By Jean Fabri and Raymond Siestrunck

Translation of "Étude de L'Hélice Supersonique." Extrait des Actes du Colloque International de Mécanique, Poitiers 1950, Vol. I. (Publications Scientifiques et Techniques du Ministère de l'Air, No. 248.)

Washington
March 1953

NATIONAL ADVISORY COMMITTEE FOR AERONAUTICS

TECHNICAL MEMORANDUM 1355

STUDY OF THE SUPERSONIC PROPELLER*

By Jean Fabri and Raymond Siestrunck

1. INTRODUCTION

The successful development of the turbojet does not necessarily entail the abandonment of the propeller at high subsonic speeds. In fact, both originate from the same principle: to furnish a thrust by increasing the momentum of the air which they pass through. While the propeller, in stirring up a large amount of air, furnishes only a slight increase of speed, the jet at the exit of the jet engine must be greatly accelerated to compensate the lack of quantity. Thus, there is a disproportion between the speed of advance and the speed of the jet which prevents the efficiency from reaching its maximum value.

This lack of proportion does not exist for the supersonic propeller; in reality, the three speeds involved in its operation - speed of air at infinity downstream, speed of air at infinity upstream, and speed of rotation - are of the same order of magnitude.

As regards the losses due to compressibility, they are especially important for the transonic speeds; by a suitable choice of the propeller dimensions so as to obtain a supersonic relative flow along the blade, these losses are likewise eliminated.

Lastly, direct mounting of the propeller on the turbine shaft gives the supersonic-turbopropeller group the simplicity that characterizes the supercharger.

2. SUMMARY ANALYSIS OF THE EFFICIENCY OF A PROPELLER-JET SYSTEM (Ref. 1)

2.1. Consider an airplane driven by a propeller and a jet simultaneously. The performance of such an aircraft, moving at forward speed V,

*"Étude de L'Hélice Supersonique." Extrait des Actes du Colloque International de Mécanique, Poitiers 1950, Vol. I. (Publications Scientifiques et Techniques du Ministère de l'Air, No. 248.)

can be characterized by the thermodynamic power

$$W_{th} = W_u' + m\frac{V^2}{2} \tag{1}$$

where W_u' is the static power furnished by the engine under identical conditions of pressure and density and m is the mass flow of fuel, and by the propulsive horsepower

$$W_p = \eta_h W_h + m''(V'' - V)V + mV^2 \tag{2}$$

where $W_h = kW_u'$ is the mechanical power absorbed by the propeller, η_h is the efficiency of the employed propeller, m'' is the total mass ejected by the jet engine, and $V'' = \lambda''V$ is the jet velocity (for simplification all velocities are assumed parallel to the forward direction).

In these conditions, the propulsive efficiency of the propeller-jet system, defined as ratio of the propulsive power to the thermodynamic power, reads

$$\eta_p = \frac{W_p}{W_{th}} = \frac{k\eta_h W_u' + V^2(m''\lambda'' - m'' + m)}{W_u' + m\frac{V^2}{2}}$$

In defining a velocity coefficient $\overline{\psi} = \frac{V}{\sqrt{\frac{2W_u'}{m}}}$, where $\frac{W_u'}{m}$, the unit horsepower of the engine, characterizes at the same time the utilized fuel and the thermal efficiency of the engine, and a dilution coefficient $\mu = \frac{m''}{m}$; the efficiency reads

$$\eta_p = \frac{k\eta_h + 2\overline{\psi}^2(\mu\lambda'' - \mu + 1)}{1 + \overline{\psi}^2}$$

As the ratio between the power absorbed by the propeller and that remaining in the jet is characterized by the relation

$$W_h + \frac{m''V''^2}{2} - \frac{(m' - m)V^2}{2} = W_u'$$

which becomes with the above notations

$$k + \bar{\psi}^2\left(\mu\lambda''^2 - \mu + 1\right) = 1$$

the propulsion efficiency takes the form

$$\eta_p = \frac{1}{1 + \bar{\psi}^2}\left[k\eta_h + 2\mu\bar{\psi}^2\left(\sqrt{\frac{1 - k}{\mu\bar{\psi}^2} + \frac{\mu - 1}{\mu}} - \frac{\mu - 1}{\mu}\right)\right] \tag{3}$$

For given conditions of flight, η_p becomes maximum when the ratio coefficient k has the value

$$k_M = 1 - \frac{\bar{\psi}^2}{\bar{\psi}_0^2}$$

with

$$\bar{\psi}_0^2 = \frac{\eta_h^2}{\eta_h^2 + \left(1 - \eta_h^2\right)\mu}$$

2.2. Example.

Consider the case of a propulsor driven at a speed of 208 m/sec (close to 750 km/h). The propeller driven by an ordinary gas turbine $\left(\frac{W_u'}{m} = 4.4 \times 10^7 \frac{kJ}{t}, \quad \mu = 60\right)$ has an efficiency of $\eta_h = 0.7$.

According to figure 1, which represents the efficiency cycle in relation to the coefficient of ratio k, the maximum efficiency differs very little from that of the propeller alone, whereas the efficiency of the jet is even lower in the contemplated conditions of flight.

This example shows that the supersonic propeller should be practical in the transonic and slightly supersonic speed range, provided that its efficiency is satisfactory ($\eta_h = 0.7$ for example), which seems to have been accomplished, according to the data given later.

For higher speeds (superspeed range), the jet engine having a higher efficiency is of greater interest.

3. GENERAL ASPECTS OF SUPERSONIC PROPELLERS

3.1. The aerodynamic study of propellers in the low-speed range has been facilitated by the identification of the helicoidal symmetry of the turbulent wake (ref. 2); reduction of the variables to two permitted the study of the performance by various methods, producing homogeneous results and confirmed by experiment (ref. 3).

No comparable test data are available in the supersonic speed range and the general equation of helicoidal potentials in compressible fluid (ref. 4) is not amenable to calculation even in its linearized form.

3.2. Being unable to compute the induced velocities, we content ourselves with approximations obtained from general considerations the use of which up to now seems justified only by reason of its simplicity.

Distinction should be made between (a) the propeller slipstream which has the effect of modifying the true incidence of the blade profiles and (b) the interference of the divers sections and particularly the effect of the tip and the hub.

The first effect, extremely important at take-off (low forward speed), must not be neglected even in normal operation. As to the second, its effect is considerably less as the relative speed, supersonic, is greater.

3.3. The performance of the propeller is characterized by the thrust coefficient

$$\tau = \frac{T}{\rho n^2 D^4}$$

the power coefficient

$$\chi = \frac{W_h}{\rho n^2 D^5}$$

and the efficiency

$$\eta_h = \frac{VT}{W_h}$$

These coefficients depend, at the same time, on the Mach number m of translation $\left(m = \frac{V}{a},\ V = \text{forward speed},\ a = \text{speed of sound in air at rest}\right)$ and on the Mach number M of rotation $\left(M = \pi n \frac{D}{a},\ n = \text{revolutions per second and } D = \text{outside diameter of propeller}\right)$.

The conventional formulas of propeller theory are generalized by taking $\lambda = \frac{m}{M}$ as performance parameter, the compressibility being characterized by M.

The following formal equations give the performance factors

$$\left.\begin{aligned} \frac{8}{\pi^2}\tau &= p\int (\xi + u)tc_z\sqrt{\lambda^2 + \xi^2}\,d\xi - p\int (\lambda + v)tc_x\sqrt{\lambda^2 + \xi^2}\,d\xi \\ \frac{8}{\pi^3}\chi &= p\int (\lambda + v)\xi tc_z\sqrt{\lambda^2 + \xi^2}\,d\xi + p\int (\xi + u)tc_x\sqrt{\lambda^2 + \xi^2}\,\xi\,d\xi \end{aligned}\right\} \quad (4)$$

where ξ is the radius of a blade section, u,v is the induced tangential and axial velocities, t is the relative chord of the particular section, and p is the number of propeller blades. (The lengths are referred to the propeller radius and the speeds to the peripheral speeds.)

4. UNIQUE SECTION METHOD

4.1. This method, which gives excellent results in the case of the classical propeller, can be adapted to the case in point. In this study, it is assumed that the performance parameter λ has a satisfactory value so that the induced velocities may be disregarded in the over-all forces, without appreciable error. In the subsequent chapter, these induced velocities are introduced in the geometric determination of the blades and in the analysis of the operating speeds at low values of λ.

Since, in order to assure satisfactory aerodynamic blade performance, the entire relative flow must be supersonic, the hub radius is always very important $\left(\xi_0 > \frac{1}{M}, \text{ where } \xi_0 \text{ is the relative hub radius}\right)$. In these conditions, the blades are small, so that $tc_z\sqrt{\lambda^2 + \xi^2}$ and $tc_x\sqrt{\lambda^2 + \xi^2}$

can be assumed constant and equal to the values in the mean blade section defined by $\xi_m = \sqrt{\frac{1 + \xi_0^2}{2}}$. Overlining these mean values and effecting the other integrations, the system (4) becomes ($u,v \sim 0$).

$$\left.\begin{aligned} \frac{8}{\pi^2}\tau &\sim \overline{ptc_z\sqrt{\lambda^2 + \xi_m^2}}\,\frac{1 - \xi_0^2}{2} - \overline{p\lambda tc_x\sqrt{\lambda^2 + \xi_m^2}}\,(1 - \xi_0) \\ \frac{8}{\pi^3}\chi &\sim \overline{p\lambda tc_z\sqrt{\lambda^2 + \xi_m^2}}\,\frac{1 - \xi_0^2}{2} + \overline{ptc_x\sqrt{\lambda^2 + \xi_m^2}}\,\frac{1 - \xi_0^3}{3} \end{aligned}\right\} \quad (5)$$

4.2. From the values of τ and χ deduced from the system (5), the propeller efficiency follows as

$$\eta_h = \pi\lambda\,\frac{\tau}{\chi} = \lambda\,\frac{\frac{1 + \xi_0}{2}\,\overline{c}_z - \lambda\overline{c}_x}{\frac{1 + \xi_0}{2}\,\lambda\overline{c}_z + \frac{1 + \xi_0 + \xi_0^2}{3}\,\overline{c}_x}$$

and, with $\overline{f}$ denoting the fineness of the mean profile

$$\eta_h = \lambda\,\frac{\frac{1 + \xi_0}{2}\,\overline{f} - \lambda}{\frac{1 + \xi_0}{2}\,\lambda\overline{f} + \frac{1 + \xi_0 + \xi_0^2}{3}} \quad (6)$$

The equation (6) shows that to each couple of values of $\overline{f}$ and ξ_0, there corresponds an optimum value of performance coefficient

$$\lambda_{opt} = -\frac{2}{3}\,\frac{1 + \xi_0 + \xi_0^2}{(1 + \xi_0)f} + \sqrt{\frac{4}{9}\,\frac{(1 + \xi_0 + \xi_0^2)^2}{(1 + \xi_0)^2 f^2} + \frac{1 + \xi_0 + \xi_0^2}{3}}$$

Figure 2 represents the variation of λ_{opt} and the corresponding efficiency plotted against $\bar{f}$ for $\xi_0 = 0.6$, and figure 3 the change in efficiency η_h against λ for $f = 8$ corresponding to a supersonic airfoil of about 6-percent thickness. It will be noted that the propeller efficiency exceeds 70 percent for $\lambda > 0.3$.

4.3. Use of theoretical polars.

In the absence of experimental data on the supersonic airfoils, recourse is had to the theoretical polars given by the linearized method

$$\bar{c}_z = \frac{4i}{\sqrt{\underline{M}^2 - 1}}$$

$$\bar{c}_x = \frac{4(i^2 + \delta^2)}{\sqrt{\underline{M}^2 - 1}}$$

where $\underline{M} = \sqrt{M^2 \xi_m^2 + m^2}$ is the relative Mach number in the mean section, i is the incidence (in radians), and where δ differs very little with the thickness of the employed profile.

In these conditions, the system (5) becomes

$$\left.\begin{aligned} \frac{8}{\pi^2}\tau &\sim \frac{4pt\sqrt{\lambda^2 + \xi_m^2}}{\sqrt{\underline{M}^2 - 1}}\left[\frac{1 - \xi_0^2}{2} i - \lambda(1 - \xi_0)(i^2 + \delta^2)\right] \\ \frac{8}{\pi^3}\chi &\sim \frac{4pt\sqrt{\lambda^2 + \xi_m^2}}{\sqrt{\underline{M}^2 - 1}}\left[\frac{1 - \xi_0^2}{2}\lambda i + \frac{1 - \xi_0^3}{3}(i^2 + \delta^2)\right] \end{aligned}\right\} \qquad (7)$$

The value of the efficiency is

$$\eta_h = \lambda \frac{\frac{1 + \xi_0}{2} i - \lambda(i^2 + \delta^2)}{\lambda \frac{1 + \xi_0}{2} i + \frac{1 + \xi_0 + \xi_0^2}{3}(i^2 + \delta^2)}$$

which, in the specified performance conditions is maximum for $i = \delta$ (profile set at incidence of maximum efficiency).

4.4. Example (similar to a case studied at the request of the S.N.E.C.M.A.).

Determination of a propeller in the following conditions:

Power absorbed . . . . . $W_n = 2080$ kW
Altitude of flight . . . . . $Z = 9000$ m
Velocity of sound . . . . . $a = 300$ m/sec
Specific mass of the air . . . . . $\rho = 4.65 \times 10^{-4}$ t/m^3
Flying speed . . . . . $V = 208$ m/s
Rate of rotation . . . . . $N = 5600$ t/mn
Diameter of hub . . . . . $D_0 = 1.33$ m

The choice of the peripheral speed determines the outside diameter, thus, for 700 m/s (or $M = 2.33$) $D = 2.39$ m, hence

$$\xi_0 = 0.56 \qquad \xi_m = 0.81 \qquad \lambda = 0.3$$

The corresponding power coefficient is

$$\chi = 0.071$$

Taking for χ the expression (7), the incidence is located at the relative chord by the following equation (profile set at incidence of maximum efficiency)

$$0.55i^2 + 0.102i - \frac{0.00124}{t} = 0$$

in the case of a propeller with six blades ($p = 6$).

Figure 4 shows the variation of the efficiency and the mean incidence plotted against the chord t.

As the relative thickness of the profile cannot fall below a certain limit, we take, for example

$$p = 6 \qquad t = 0.168 \qquad i = \delta = 0.067(3.8^\circ)$$

hence

$$T = 700\text{kg} \quad \text{and} \quad \eta_h = 0.70$$

5. CORRECTION FOR SLIPSTREAM

5.1. In the absence of an exact method of evaluating the velocities induced by the free vortices, a generalized approximation of that used for the conventional propellers is applied.

Limiting the study to propellers with subsonic forward speed ($m < 1$), the absolute speed is subsonic at every point. And then it can be assumed that the evaluation of the induced velocities is similar to that observed on ordinary propellers, and particularly, to those which assume, in the propeller plane, a value half of that assumed at infinity downstream in the wake.

Applying the classical reasoning gives, in this case, the usual values

$$u = -\frac{p\Gamma}{4\pi\xi} \qquad v = \frac{p\Gamma}{4\pi\lambda^*} \tag{8}$$

$\Gamma = \frac{tc_z\sqrt{\lambda^2 + \xi_m^2}}{2}$ being the circulation of the mean section and

$\lambda^* = \xi\,\frac{\lambda + v}{\xi + u}$ the real speed of the streamline at the crossing of the plane of the propeller.

The axial velocity v, very important at the fixed point, is involved in all conditions for the determination of the setting; whereas, the tangential velocity u is generally negligible, hence

$$\lambda^* \sim \lambda + v$$

5.2. Operation at the fixed point.

The induced velocities are very important in the study of fixed point operation ($\lambda = 0$, $\underline{M} = M\xi$). In calling $\hat{\lambda}$ the particular value of λ^* corresponding to the fixed point, $\hat{\lambda} \sim v$, according to equation (8)

$$\hat{\lambda} = \sqrt{\frac{p\Gamma}{4\pi}} = \sqrt{\frac{pt\xi_m c_z}{4\pi}}$$

and the system (7) becomes

$$\left.\begin{aligned} \frac{8}{\pi^2}\tau &\sim \frac{4pt\overline{\xi_m}}{\sqrt{M^2-1}}\,\frac{1-\xi_0^2}{2}\,i \\ \frac{8}{\pi^3}\chi &\sim \frac{4pt\overline{\xi_m}}{\sqrt{M^2-1}}\left[\frac{1-\xi_0^2}{2}\sqrt{\frac{pt\overline{\xi_m}}{2\pi\sqrt{M^2-1}}}\,i^{3/2} + \frac{1-\xi_0^3}{3}\left(i^2+\delta^2\right)\right] \end{aligned}\right\} \qquad (9)$$

5.3. Example[1].

Performance of supersonic propeller at the fixed point:

Power absorbed . . . . . $W_h = 74$ kW
Rate of rotation . . . . . $N = 12000$ rpm
Speed of sound . . . . . $a = 340$ m/s
Air density . . . . . $\rho = 12.25 \times 10^{-4}$ t/m^3

Taking $M = 2$ and $\xi_0 = 0.6$ we get

Outside diameter . . . . . $D = 1.08$ m
Power coefficient to be realized . . . . . $\chi = 0.00514$

The results obtained with a two-blade propeller are given in figure 5; since the thickness of the profile cannot drop below 0.06, the two-blader is defined by

$$t = 0.1 \qquad i = \delta = 0.061(3.5^\circ)$$

which is most interesting.

5.4. Setting of profiles.

The induced velocities determine the setting of the profiles. In fact, incidence i, setting α and performance parameter λ are limited by the relation

$$i = \alpha - \arctan\frac{\lambda}{\xi} - \frac{v}{\xi} \qquad (10)$$

[1]This case corresponds to tests contemplated; the propeller is to be driven by a Turbomeca gas turbine.

Thus, in the example 4.4, the induced velocity, the root of the equation

$$v = \frac{p\Gamma}{4\pi(\lambda + v)}$$

or

$$v^2 + \lambda v + i\,\frac{pt\sqrt{\lambda^2 + \xi_m^2}}{2\pi\sqrt{\underline{M}^2 - 1}} = 0$$

shifts the setting from

$$\alpha = i + \text{arc tan}\,\frac{\lambda}{\xi} = 23.94^\circ$$

to

$$\alpha = i + \text{arc tan}\,\frac{\lambda}{\xi} + \frac{v}{\xi} = 25.12^\circ$$

Similarly, in example 5.3, the setting is

$$\alpha = i + \frac{\hat{\lambda}}{\xi} \sim 5.9^\circ$$

instead of

$$i = 3.5^\circ$$

if the induced velocities are neglected.

5.5. Performance curves.

We are now prepared to study the performance curves of a given propeller as function of λ, M and setting α (a supersonic propeller must, of course, be of the variable pitch type). It is sufficient to join to the system (7) the relations

$$i = \alpha - \text{arc tan}\,\frac{\lambda}{\xi_m} - \frac{v}{\xi_m}$$

$$v = i\,\frac{pt\sqrt{\lambda^2 + \xi_m^2}}{2\pi(\lambda + v)\sqrt{\underline{M}^2 - 1}}$$

which combined give an equation of the second degree defining the incidence and the induced axial velocity. Figure 6 shows the variation in relation to λ, τ, χ, and η_h for the case of the propeller 4.4, near its design conditions.

6. INTERFERENCE OF DIVERS SECTIONS

6.1. Effect of tip and of hub.

Aside from the velocities induced by the slipstream, the interference of various sections must also be taken into consideration. This interference, due to the nonuniformity of the flow, has no appreciable effect except at the blade tip and near the hub.

There is no exact theory on the interference of blade sections, but the following considerations make it possible to determine the order of magnitude of the corresponding correction (ref. 5).

It should be noted that, since the relative flow is supersonic, any disturbance created at one point is transmitted only to the inside of a zone of action, the characteristic conoid of the equation satisfied by the potential of perturbation.

In addition, the method of load distribution over a lifting surface in supersonic translation (ref. 6), which gives satisfactory results for rectangular wings, is also generalized. By considering only blades with leading edge normal to the relative sound (a nonrestrictive condition which is a result of the form imposed by the strength of the materials), it is assumed that any local variation of the slope of the contour of each profile induced inside of the characteristic conoid of flow issues from the point considered; value of the velocity is supplied by the two-dimensional theory of forward flow, the Mach number of the comparative flow being, of course, the Mach number of the profile in its relative motion. The pressure at a point is the mean of the pressures corresponding to the velocities induced by all the disturbances sent out to the inside of its characteristic forecone: the pressure coefficient at the point (ξ, η) of the blade is given by

$$c_p \sim \int_{-\infty}^{\eta} \frac{d\eta}{\xi_1 - \xi_2} \int_{\xi_1}^{\xi_2} \frac{2}{\sqrt{M^2 - 1}} \frac{\partial \delta}{\partial \eta} d\xi \qquad (11)$$

where $\underline{M} = \sqrt{M^2\xi^2 + m^2}$, $\delta(\xi,\eta)$ denote the slope of the profile contour and $\xi_1 - \xi_2$ the parallel portion at the leading edge comprises the coordinate η at the inside of the characteristic forecone of the point in question.

6.2. Zone of influence.

As said before, a disturbance sent forth makes itself felt only at the inside of the characteristic cone of this point. Using the mean camber line of the blades as reference surface, the limit of the zone of influence can be defined as the curve forming in each point the Mach angle, arc sin $1/\underline{M}$ with the velocity. This limit is thus defined as integral curve of the differential equation

$$\frac{d\eta}{d\xi} = \pm\sqrt{M^2\xi^2 + m^2 - 1}$$

passing through the particular point, that is

$$(c_1)_{2\eta_1} = \xi_1\sqrt{M^2\xi_1^2 + m^2 - 1} - \xi\sqrt{M^2\xi^2 + m^2 - 1} + \frac{m^2 - 1}{M}\log\frac{M\xi_1 + \sqrt{M^2\xi_1^2 + m^2 - 1}}{M\xi + \sqrt{M^2\xi^2 + m^2 - 1}}$$

$$(c_2)_{2\eta_2} = \xi\sqrt{M^2\xi^2 + m^2 - 1} - \xi_1\sqrt{M^2\xi_1^2 + m^2 - 1} + \frac{m^2 - 1}{M}\log\frac{M\xi + \sqrt{M^2\xi^2 + m^2 - 1}}{M\xi_1 + \sqrt{M\xi_1^2 + m^2 - 1}}$$

Figure 7 represents the family of characteristic curves corresponding to the following conditions

$$M = 2.33 \qquad m = 0.7$$

It is readily seen that the interference assumes significance only for slightly supersonic speeds.

6.3. Corrections for nonuniform flow.

The integral (11) represents the mean value of c_p in the characteristic forecone of the point (ξ,η). The relative Mach number being a uniformly increasing function of ξ and the slope variations remaining small, this mean value of c_p differs very little from the value of c_p in the medium section; that is, in all sections that are not influenced by the blade tips, the pressure coefficient can be computed as if that section were located in a two-dimensional flow of Mach number $\underline{M} = \sqrt{M^2\xi^2 + m^2}$.

6.4. Effect of free blade tip.

The decrease in lift at the blade tip ($c_z = 0$ for $\xi = 1$) is taken into consideration by a generalization of the classical method of images, that is, by extending the blade by a symmetric fictitious geometric surface of the mean camber line of the blade with respect to the relative upstream velocity of the marginal section and placed with the incidence opposite to that of the blade in a flow of Mach number $\underline{M} = \sqrt{M^2(2 - \xi)^2 + m^2}$.

This reduces the problem to that of considering fictitious pressure coefficients at the inside of the marginal characteristic conoid corresponding to this new lifting surface and additive to the real pressure coefficients due to the velocities induced by the blade itself.

With + referring to quantities relating to top camber and - to bottom camber, this fictitious lifting surface is defined by

$$\delta^+ = \delta^- = i - \frac{\theta_+ + \theta_-}{2}$$

the incidence i and the local slopes θ_+ and θ_- being measured in the symmetrical section of the particular section with respect to the tip of the blade.

6.5. Effect of hub.

A similar image takes care of the condition at the hub; that is, due to the fact that the radial velocities cancel out for $\xi = \xi_0$, the blade is prolonged by a fictitious wing defined by

$$\delta(\xi) = \delta(2\xi_0 - \xi)$$

that is, symmetrical to the blade with respect to the plane of the hub section, the upstream Mach number being defined by

$$\underline{M} = \sqrt{M^2(2\xi_0 - \xi)^2 + m^2}$$

The local pressure coefficient is obtained by adding the pressure coefficients induced by the fictitious wing to those induced by the blade itself, in the characteristic conoid of the hub section.

6.6. Calculation of c_z and c_x.

Knowing the pressure coefficients, the lift and drag coefficients are easily obtained

$$\left.\begin{aligned} c_z &= \frac{1}{t}\int_0^t (c_{p_-} - c_{p_+})d\eta \\ c_x &= \frac{1}{t}\int_0^t (c_{p_+}\delta_+ - c_{p_-}\delta_-)d\eta \end{aligned}\right\} \qquad (12)$$

which, entered in equation (7) give the thrust and power coefficients.

Of course, these corrections must be made before calculating the velocities induced by the free vortices. As pointed out in the foregoing, the purpose of this approximate method is solely to determine the order of magnitude of the corrections and hence to justify the unique section method.

6.7. Example.

The correction which we have in view is of interest only if it is easy to compute; besides, the integrals (12) are replaced by general formulas generalizing those obtained by the same method on wings in uniform flow (ref. 6). It should be noted that only the lift correction is of interest, the drag correction being rather much less.

To illustrate, the effect of the free tip is expressed by

$$c_z = \frac{4i(1 - \xi)}{t}\left[1 - \log \frac{(1 - \xi)\sqrt{\underline{M}^2 - 1}}{t}\right]$$

for

$$1 - \frac{t}{\sqrt{M^2 - 1}} < \xi < 1$$

In the part not disturbed by the tips we simply get

$$c_z = \frac{4i}{\sqrt{M^2 - 1}}$$

As regards the effect of the reflection on the cylindrical wall of the hub, it is relatively unimportant and the approximate limit value is simply written as

$$c_z = \frac{4i_0}{\sqrt{M^2\left(\xi_0 + \frac{t}{3\sqrt{M^2\xi_0^2 + m^2 - 1}}\right)^2 + m^2 - 1}}$$

with

$$i_0 = i\left(\xi_0 + \frac{t}{3\sqrt{M^2\xi_0^2 + m^2 - 1}}\right)$$

Figure 8 shows the evolution of the lift coefficient obtained by this method, by comparing it to the c_z of the two-dimensional method, in the case of the propeller 4.4, where $\lambda^* \sim \lambda + v$ was assumed constant over the blade, the setting of the profiles being such that the incidence is constant and equal to 4°.

7. CONCLUSION

This study of the supersonic propeller is merely an attempt to determine the order of magnitude and the direction of variation of the performance characteristics.

The results obtained indicate that, in a reasonably wide speed range (transonic and slightly supersonic), the propulsive efficiency of the supersonic propeller can be as high as 70 percent, at least, when assuming that the airfoil characteristics are comparable for rotation and for translation.

To be sure, the mechanical difficulties should not be underestimated, particularly those concerned with pitch-changing devices as well as those arising from high rotational speeds.

Nevertheless, direct mounting of the supersonic propeller on the turbine shaft is possible and the propeller can certainly provide appreciable service in the propulsion range considered.

Tanslated by J. Vanier
National Advisory Committee
for Aeronautics

REFERENCES

1. Roy, M.: Thermodynamique des systèmes propulsifs à réaction. Cours professé au C.E.S.M., Dunod, Paris, 1947.

2. Siestrunck, R.: Le développement moderne de la théorie de l'hélice. Gauthier-Villars, Paris, 1947.

3. Siestrunck, R.: Écoulements à potentiel dans les machines hélicoïdales simples, O.N.E.R.A., 32, Paris, 1949.

4. Siestrunck, R., and Fabri, J.: Sur l'équation générale des potentiels hélicoïdaux en fluide compressible. Comptes rendus Académie des Sciences, 226, 1948, p. 1430.

5. Siestrunck, R., and Fabri, J.: Détermination approachée des corrections dues aux vitesses induites dans les machines axiales à vitesse relative supersonique. Comptes rendus Académie des Sciences, 226, 1948, p. 1795.

6. Fabri, J.: Sur une méthode approchée de calcul des répartitions de charges sur des surfaces portantes à bord d'attaque supersonique. Comptes rendus Académie des Sciences, 226, 1948, p. 1172.

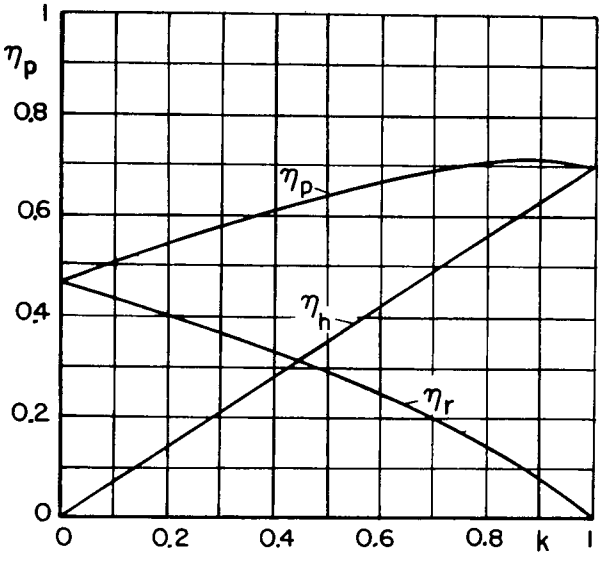

Figure 1

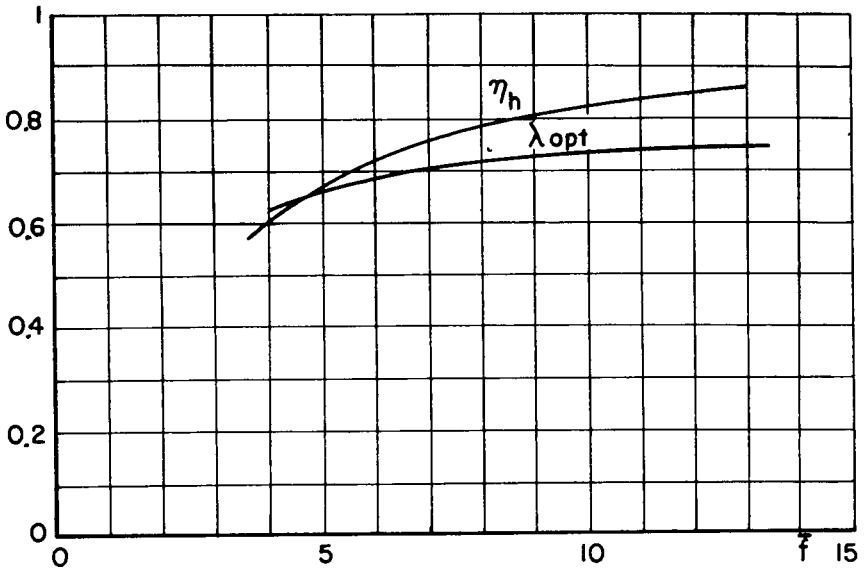

Figure 2

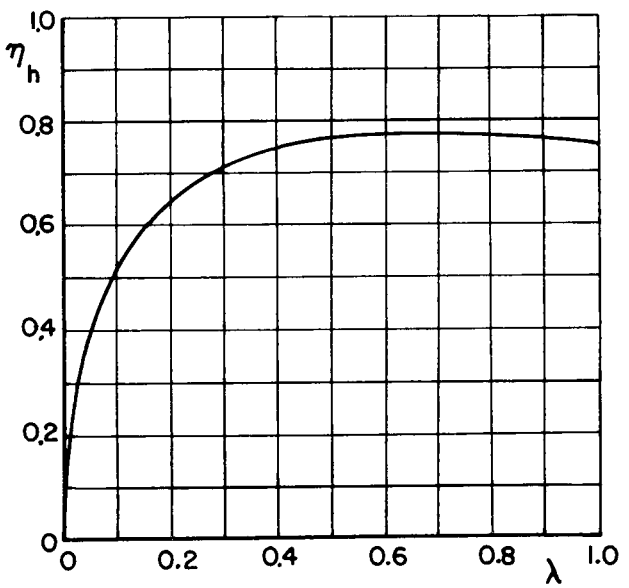

Figure 3

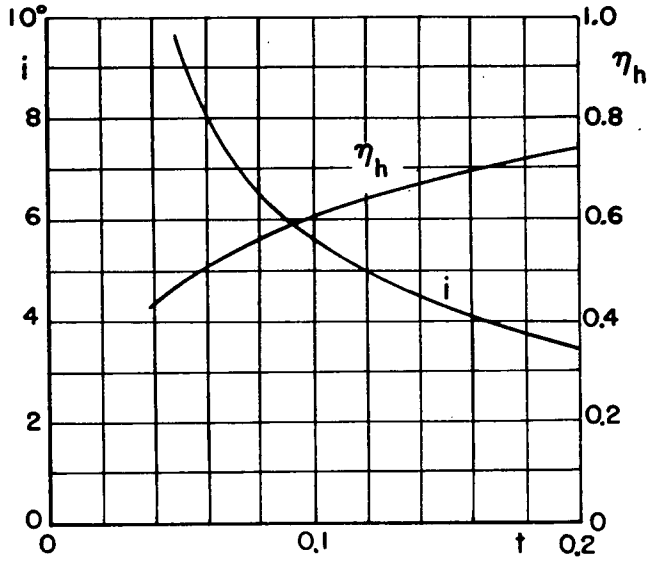

Figure 4

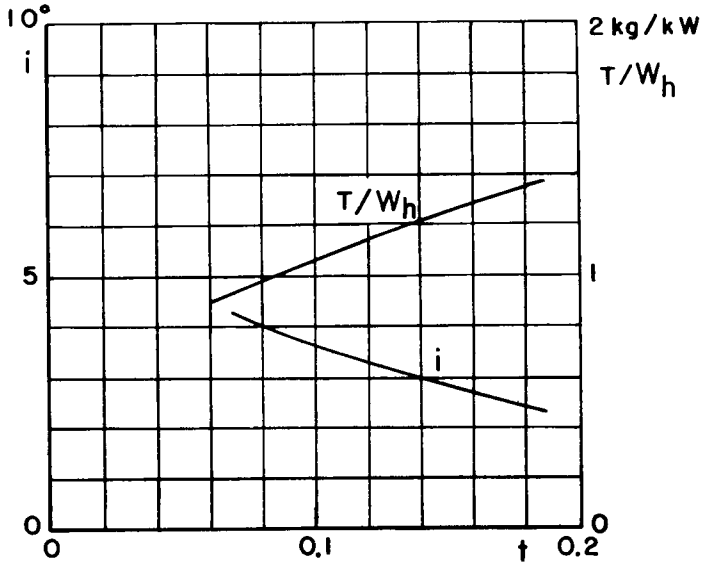

Figure 5

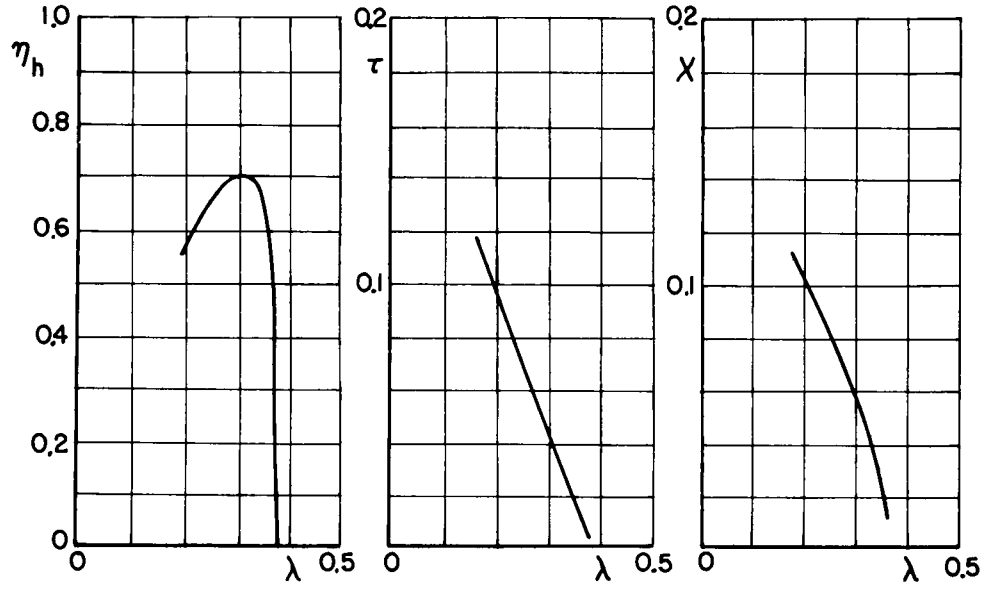
1.0
η_h
0.8
0.6
0.4
0.2
0
0
λ
0.5
0.2
τ
0.1
0
λ
0.5
0.2
χ
0.1
0
λ
0.5

Figure 6

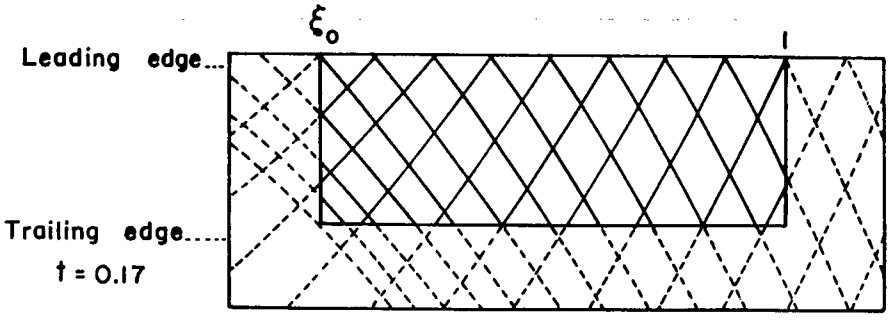

Figure 7

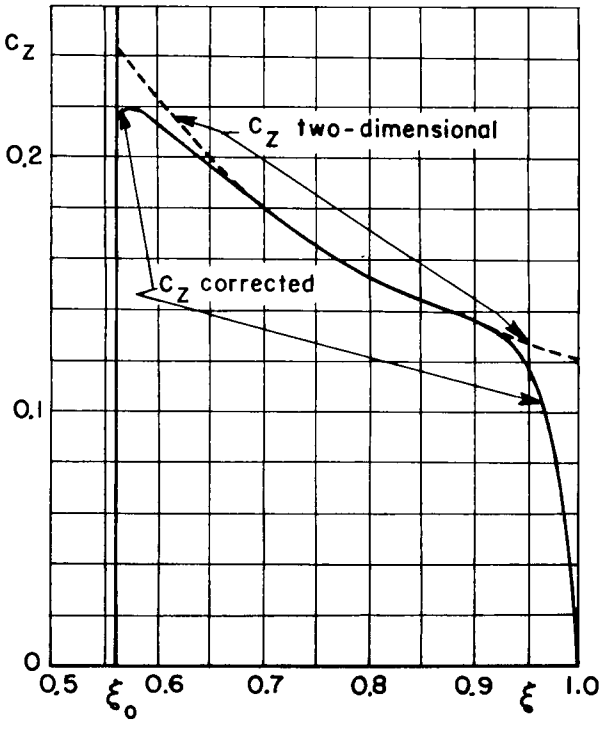

Figure 8

NACA-Langley - 3-13-53 - 1000